

**The Influence of the Quasi-Biennial Oscillation on the
Troposphere in Wintertime in a Hierarchy of Models, Part
2-Perpetual Winter WACCM runs**

CHAIM I. GARFINKEL * DENNIS L. HARTMANN

Department of Atmospheric Science, University of Washington, Seattle, WA

* *Corresponding author address:* Department of Atmospheric Science, University of Washington, Seattle, WA 98195.

E-mail: cig4@atmos.washington.edu

ABSTRACT

Experiments with the Whole Atmosphere Community Climate Model (WACCM) are used to understand the influence of the stratospheric tropical Quasi-Biennial Oscillation (QBO) in the troposphere. The zonally symmetric circulation in thermal wind balance with the QBO affects high frequency eddies throughout the extratropical troposphere. The influence of the QBO is strongest and most robust in the North Pacific near the jet exit region, in agreement with observations. Variability of the stratospheric polar vortex does not appear to explain the effect that the QBO has in the troposphere in the model, though it does contribute to the response in the North Atlantic. Anomalies in tropical deep convection associated with the QBO appear to damp, rather than drive, the effect of the QBO in the extratropical troposphere. The thermal wind response to QBO momentum anomalies interacting with tropospheric transient waves appears to be the crucial mechanism through which the QBO produces significant anomalies in the extratropical troposphere. The response to QBO winds of realistic amplitude is stronger for perpetual February radiative conditions and sea surface temperatures than perpetual January conditions, consistent with the observed response in reanalysis data, in a coupled seasonal WACCM integration, and in dry model experiments described in part 1.

1. Introduction

Stratospheric anomalies have been shown to affect the wintertime tropospheric circulation. In particular, variability of the stratospheric polar vortex is linked with the Northern Annular Mode (NAM)(Baldwin and Dunkerton 1999; Polvani and Kushner 2002; Limpasuvan et al. 2004). Even though the equatorial stratospheric QBO is the dominant mode of inter-annual stratospheric variability in the Tropics, its affect on the wintertime tropospheric circulation has been less thoroughly investigated.

Crooks and Gray (2005), Coughlin and Tung (2005), and Haigh et al. (2005) find that the anomalous QBO winds seemingly curve downwards in a horseshoe shaped pattern into the subtropical troposphere, with wind anomalies of opposite sign in the deep Tropics and extratropics (see also Figure 6 of Giorgetta et al. (1999), Figure 6 of Garfinkel and Hartmann (2010), and Figure 2 of Garfinkel and Hartmann (2011)). The signal is especially strong in February and March in the North Pacific. Figure 1 shows the difference in 300hPa zonal winds between easterly QBO and westerly QBO composites in the ECMWF reanalysis (Uppala et al. 2005) and in a coupled WACCM integration. The QBO appears to have a robust influence in the troposphere in both, whereby lower stratospheric easterlies lead to a weaker subtropical tropospheric jet in the North Pacific (hereafter NP). How this signal is communicated downwards through the tropopause has not been fully established however.

We consider three possible mechanisms. The first mechanism is that once the anomalous QBO winds influence the strength of the stratospheric polar vortex (Holton and Tan 1980; Baldwin et al. 2001; Coughlin and Tung 2001; Ruzmaikin et al. 2005; Marshall and Scaife 2009), it can then affect the troposphere just like any polar vortex anomaly. While this

vortex mechanism is likely important for the response in the North Atlantic, Garfinkel and Hartmann (2010) find that the response to the QBO in the NP is qualitatively different from the influence of the polar vortex in the NP. Some additional mechanism must be present for a complete explanation of the effect of the QBO in the troposphere.

In the second and third mechanisms considered, the meridional circulation that maintains thermal wind balance with QBO equatorial stratospheric wind anomalies interacts with the troposphere. See section 4 of Garfinkel and Hartmann (2011) (hereafter Part 1) and references therein for a full discussion of this meridional circulation. Briefly, this circulation includes (1) rising motion and a cold temperature anomaly near the equator and sinking motion and warm temperature anomalies near 30° in the lowermost stratosphere, and (2) arching of QBO wind anomalies downwards to the troposphere and polewards to near 20° . Even though this meridional circulation penetrates the tropopause only weakly, this circulation can affect tropospheric variability in (at least) two ways.

If the meridional circulation of the QBO can modulate tropical deep convection (Giorgetta et al. 1999; Collimore et al. 2003), it can affect the local Hadley circulation and the extratropics as well. Ho et al. (2009) suggest that such a change in tropical convection affects NP summertime tropical cyclone tracks. Demonstrating a connection between anomalies in convection and the QBO in winter in the observational record is difficult, however. Over the past three decades, when reliable satellite observations of outgoing longwave radiation (OLR) are available, westerlies in the lowermost equatorial stratosphere and El-Niño have tended to coincide (Garfinkel and Hartmann 2007)¹. The difference in OLR between com-

¹In contrast, EQBO and El-Niño tended to coincide from 1957 to the start of the satellite era. The average Niño3.4 index for the composites used in Figure 1a, which sample from 1957 to 2007, are within

posites of WQBO and EQBO events therefore resembles the difference between El Niño and La Nina (not shown). It is not clear whether the QBO would modulate wintertime tropical convection, and thermally driven subtropical jets, under fixed sea surface temperatures (SSTs). Furthermore, Part 1 showed that the QBO can influence the troposphere in a model that lacks realistic polar vortex variability and convection, implying that these are not the sole pathways through which the QBO can influence the troposphere.

Finally, the meridional circulation of the QBO can influence extratropical tropospheric eddies directly and thereby bias the troposphere towards its leading modes of variability. Part 1 showed that in the presence of tropospheric variability, eddies amplify the zonal wind anomalies that would exist in the absence of eddies. Even though the results of part 1 are consistent with observations, the simplified model used there does not include convection or vortex variability. We therefore explore the tropospheric response to the QBO in a more realistic model configuration.

The primary tools used are perpetual January and February Whole Atmosphere Community Climate Model (WACCM) runs with fixed SSTs. WACCM runs with a neutral QBO stratospheric wind profile are compared to runs with an easterly QBO(EQBO) stratospheric wind profile. Because the SSTs are fixed, our model runs cleanly isolates the influence that the QBO may have on parametrized convection. Because our model also has a variable polar vortex, the influence of the QBO on the troposphere through its effect on the vortex is simulated as well. By understanding how the QBO affects the troposphere in these model runs, the mechanism(s) through which the QBO affects the troposphere in observations can be elucidated.

0.15 of each other. The significant anomaly in Figure 1a is not due to aliasing from El-Niño.

Section 2 introduces the model used and Section 3 discusses some aspects of the control run. Section 4 discusses the response to imposing EQBO stratospheric winds and the role of high frequency eddies for the amplifying the tropospheric response. Section 4a shows that convection and vortex variability do not explain the effect of the QBO in the extratropical troposphere. Section 4b shows that the model results are robust to model configuration.

2. The Model

Perpetual January and February simulations are used to investigate the response to QBO stratospheric wind anomalies. WACCM version 3.1.9 (Marsh et al. 2007; Garcia et al. 2007) is run with fixed SSTs, land surface and ice, perpetual January 15th or February 5th radiative forcing, the Zhang and McFarlane (1995) convection scheme as implemented in CAM3 (Collins et al. 2006), and with interactive chemistry turned off. The horizontal resolution is 4° latitude by 5° longitude, and the model has 66 vertical levels (a hybrid sigma-vertical coordinate) extending into the thermosphere.

a. QBO relaxation

The QBO wind relaxation is like Matthes et al. (2010)(see references therein). Between model layers 0.0026 and 0.08565 (approximately 2.6hPa and 85.7hPa), the winds at the equator are linearly relaxed towards the specified profile with a 10 day timescale. At model level 0.1005 (approximately 100.5hPa), the relaxation timescale at the equator is 20 days. Away from the equator, the linear relaxation timescale increases as $\tau(\phi) = \tau_{eq} e^{\frac{1}{2}(\frac{\phi}{10^\circ})^2}$ days,

where ϕ is latitude and τ_{eq} is the relaxation timescale at the equator. Winds evolve freely poleward of 22° latitude.

The default EQBO wind profile is similar to, though slightly stronger than, a typical EQBO wind profile, and is the same wind profile used in Garfinkel and Hartmann (2010) and part 1. Unlike real EQBO wind profiles, the profile relaxes to climatological easterlies in the upper stratosphere. Section 4b shows that sensitivity to the upper stratospheric wind anomalies is weak. To demonstrate the realism of the magnitude of the EQBO wind anomalies, asterisks on Figure 2 denote the 5% – 95% range of QBO variability of the equatorial winds from May 1953 to April 2007; our EQBO profile is within the natural variability of QBO profiles. Huesmann and Hitchman (2001) and Collimore et al. (2003) define an event by a 1.5m/s shear per 20hPa between 50hPa and 70hPa. The difference in the zonal wind relaxed towards between these two levels is 11.3m/s. Our lower stratospheric shear is stronger than a typical event in Huesmann and Hitchman (2001) but still within the natural variability (see Figure 6 of Huesmann and Hitchman (2001)).

b. Methodology

The runs are initialized by first running WACCM with the full seasonal cycle for at least one year. Perpetual January 15th (or February 5th) conditions are then imposed, and equatorial stratospheric winds are relaxed to the climatological equatorial stratospheric winds from May 1953 to April 2007 (dashes in Figure 2). The model integration is then continued for at least an additional 235 months, of which the first 10 months are discarded. These constitute our January and February control runs, denoted JCONT and FCONT on

Table 1.

Two types of EQBO runs are explored. In the first type we (1) branch off the instantaneous atmospheric state at the beginning of each month of the control runs, (2) impose an EQBO wind profile, and then (3) integrate each ensemble member for an additional 120 days. Because the relaxation timescale for the QBO winds is no faster than 10 days, the atmosphere can smoothly adjust to the EQBO equatorial stratospheric profile. We thus generate a large ensemble of the transient NP response to EQBO winds. We focus on the transient response rather than the equilibrated steady state response (1) because the transient response allows us to investigate the causality more cleanly, and (2) because the response to the QBO in observations will never reach equilibrium due to the seasonal cycle, implying that the transient response is more relevant to the observed response. We focus on the response in the troposphere in February with a three times stronger EQBO (hereafter 3x EQBO) profile to show the response in the troposphere more clearly (FBRANCH on Table 1), but also mention results in perpetual January with the default EQBO profile (JBRANCH on Table 1).

The second type of runs are long quasi-steady equilibrium runs in which the EQBO relaxation is always present (see Table 1). The runs are used to explore sensitivity of our results to the EQBO profile chosen and to the choice of perpetual February as opposed to perpetual January. In the first run, the 3x EQBO profile is used. In the second, the default EQBO profile is used; in the third, the EQBO profile includes upper stratospheric westerlies (triangles on Figure 2). In the fourth, lower stratospheric winds are relaxed towards a weak EQBO profile, while winds below model level $\sigma=0.0615$ are relaxed towards the neutral QBO profile; the resulting QBO perturbation is weaker than many observed QBO events and localized to the lower stratosphere (pluses on Figure 2). In the fifth, we attempt

to mimic the internally generated QBO in some recent climate models (e.g. Giorgetta et al. (2006), Anstey et al. (2010), Kulyamin et al. (2009), Kawatani et al. (2010), and Osprey et al. (2010)). In many of these models the QBO winds are too weak or do not extend strongly enough below 50hPa. To mimic such a QBO, we relax to a weak sheared EQBO profile only above model level $\sigma=0.0615$ (diamonds on Figure 2).

Any robust differences between the control case and the EQBO case in the midlatitudes or in the troposphere are part of the response to the EQBO relaxation, rather than due to the relaxation itself. Because the QBO relaxation method here and in Part 1 are identical, the meridional circulation discussed at length in Section 4 of Part 1 is assumed to exist in the WACCM runs shown here. This assumption will be verified in Section 4. Significance is determined by a 2 tailed Student-t difference of means test.

c. Vorticity Budget

Part 1 found that transient eddies are crucial for amplifying the tropospheric response to the QBO. It is therefore important to diagnose, in our model runs, the role of transient eddies in providing the vorticity fluxes that amplify the tropospheric response and extend it downwards to the surface. Barnes and Hartmann (2010a)(hereafter BH10) and Barnes and Hartmann (2010b) show that eddy feedbacks in zonally confined regions can be diagnosed quantitatively by using the vorticity budget:

$$\begin{aligned}
\frac{\partial \hat{\zeta}}{\partial t} = & \left[-(\bar{\zeta} + f)\nabla \cdot \hat{\mathbf{u}} - \hat{\zeta}\nabla \cdot \bar{\mathbf{u}} \right]_{\text{stretching}} + \left[-\nabla \cdot (\hat{\mathbf{u}}\hat{\zeta}) \right]_{\text{eddy}} \\
& + \left[-\hat{\mathbf{u}} \cdot \nabla(\bar{\zeta} + f) - \bar{\mathbf{u}} \cdot \nabla\hat{\zeta} \right]_{\text{wave}} + \left[-\nabla \cdot (\bar{\mathbf{u}}(\bar{\zeta} + f)) \right]_{\text{clim}} \\
& - \left[(\hat{\omega} + \bar{\omega})\frac{\partial(\hat{\zeta} + \bar{\zeta})}{\partial p} + \hat{\mathbf{k}} \cdot \left[\frac{\partial(\hat{\mathbf{u}} + \bar{\mathbf{u}})}{\partial p} \times \nabla(\hat{\omega} + \bar{\omega}) \right] \right]_{\text{vert}} + \mathcal{F}.
\end{aligned} \tag{1}$$

BH10 argue that when the vorticity forcing terms in upper levels project onto vorticity anomalies in lower levels, lower level vorticity anomalies can be maintained against damping. See BH10 for more details.

The vorticity budget is used here to diagnose the role of transient tropospheric eddies in the tropospheric response to the QBO. The terms in the vorticity budget are computed for the FCONT run and FBRANCH ensemble, with the mean state from the FCONT run used for both. High frequency eddies are separated by a 9th order Butterworth filter with a 7 day cutoff, like in Part 1. The difference in the forcing terms between FCONT and the FBRANCH ensemble diagnoses the generation of zonally asymmetric tropospheric vorticity anomalies.

3. Mean State and Variability of the Control Runs

Before we analyze the response to QBO winds in our model, we first explore the fidelity of the mean state and variability of the control runs. Figure 3 compares the time mean zonally averaged zonal wind and temperature of the JCONT runs to the January mean state in the ECMWF reanalysis. In the Northern Hemisphere(NH), jets below 25km are in the correct location and have the correct magnitude in the JCONT (and FCONT) runs. In the Southern Hemisphere(SH), however, disagreements are larger. The SH stratosphere has easterlies everywhere in the reanalysis, but in the JCONT run a weak vortex is present near the pole. The polar lowermost SH stratosphere is too cold, and the SH tropospheric jet is too strong, in JCONT as compared to the reanalysis. Biases in FCONT are even larger than biases in JCONT. The lack of fidelity between the SH mean state of the WACCM runs

and the reanalysis indicates that the results for the SH should be regarded with caution, particularly if the stratospheric summer easterlies are regarded as important. The direct downward effect in the Tropics is likely not strongly affected by these biases, however.

Though the NH mean state of the WACCM is similar to observations, WACCM v3.1.9 has too little stratospheric polar vortex variability and too few sudden stratospheric warmings. The standard deviation of temperature area averaged from 70N and poleward and 70hPa to 150hPa (i.e. lower stratospheric polar cap temperature) is 3.5K in JCONT, while it is 4.2K from 1958 to 2007 in the ECMWF reanalysis. A similar bias is present in FCONT. Such reduced variability might bias our conclusions on whether the QBO can influence the troposphere via the vortex. To show that this is likely *not* the case, we compare the influence of the QBO on the lowermost stratosphere in the reanalysis to the WACCM runs. The difference in polar cap temperature between our equilibrium EQBO January runs and JCONT is 1.15K, which is comparable to the difference between a reanalysis EQBO composite and climatology over these pressure levels in winter. Changes in EP flux are broadly consistent with the Holton-Tan mechanism (Garfinkel et al. 2011). Only higher in the stratosphere is the influence of the QBO on polar cap temperatures greater in the reanalysis than in our WACCM runs. As the influence of polar vortex variability on the troposphere is communicated through the lower stratosphere, we expect that our WACCM runs capture reasonably well the ability of the QBO to influence the troposphere by first influencing the vortex.

Part 1 found that QBO winds incline a tropospheric jet towards one phase of its dominant mode of variability, but that the direction that the jet shifts depends on properties of the mean state and modes of variability of the jet. In particular, a jet whose dominant mode of variability is north-south shifting shifts *poleward*, with the poleward shift stronger for a jet at

30N than a jet at 40N. A strong subtropical jet whose dominant mode of variability resembles pulsing of the jet shifts responds weakly to QBO winds. We therefore explore the dominant modes of lower tropospheric variability of the JCONT and FCONT runs ². An EOF analysis is performed for $\sqrt{\cos\phi}$ weighted daily zonal wind variability at 925hPa over the North Pacific region(20N and poleward, 150E to 150W), North Atlantic(20N and poleward, 60W to 0E), and the Southern Hemisphere from 20S and poleward. The autocorrelation of the first and second principal component is computed, and the portion of the autocorrelation function above 1/e is fit to a decaying exponential. The e-folding timescale of this decaying exponential and the variance explained by the EOF is listed in Table 2.

The first EOF in the SH resembles the Southern Annular Mode (SAM; not shown) and is well separated from the second EOF. The long timescale for the first EOF is consistent with the presence of eddy feedback for a shifting jet(Lorenz and Hartmann 2001; Barnes and Hartmann 2010b)³. The second SH EOF is not well separated from the third. In the Atlantic sector, the first and second EOF are well separated from each other and from the third EOF, and indicate shifting(i.e. NAO) and pulsing of the jet respectively(not shown).

²Because lower tropospheric variability more cleanly isolates the influence of high frequency eddies rather than the influence of the thermal component of the Hadley circulation, we focus on lower levels.

³In the SH, the FCONT jet is further poleward yet its jet shifts persist for longer than those of the JCONT jet. That a further poleward jet would have stronger eddy feedback seemingly contradicts Barnes et al. (2010) where more poleward jets have weaker eddy feedbacks and smaller jet-shifting persistence timescales. One possible explanation is that the weak yet variable stratospheric polar vortex in FCONT couples to tropospheric variability while the even weaker vortex in JCONT does not (not shown). Coupling between the lowermost stratosphere and troposphere has been shown to increase the persistence timescale of tropospheric annular modes (Gerber and Polvani 2009). A thorough investigation is outside the scope of this work.

We therefore expect a poleward jet shift via the SAM and NAO if our dry model results are relevant to WACCM.

In the Pacific sector, the first EOF resembles a shifting jet for FCONT and hybrid pulsing-shifting for JCONT, like in Eichelberger and Hartmann (2007) (see Figure 4a,c)⁴. The difference in lower tropospheric first EOFs suggests stronger transient eddy feedback in FCONT than in JCONT. We therefore might expect a slightly stronger response in the North Pacific to EQBO winds in February, if the intuition from part 1 is relevant.

The jets examined in part 1 were highly idealized however, while the jets examined here are much more realistic. The first EOF (the annular mode) dominates the variability in a dry model unrealistically, while both pulsing and shifting of the jet are present and contribute to Pacific sector jet variability. In addition, the jets examined here have realistic zonal asymmetry, unlike the jets in part 1. Finally, the mean state of the FCONT and JCONT runs are much more similar (e.g. the subtropical NP jet maximum is only ~ 5 m/s greater in JCONT than FCONT) than the mean state of the strong and weak subtropical jets from part 1. We therefore test, in the rest of this paper, whether and how EQBO winds influence realistic tropospheric jets.

4. Tropospheric Response to EQBO winds

The response in the troposphere to the inclusion of EQBO tropical stratospheric winds is now explored. We first explore the response in an ensemble of runs in which 3x EQBO

⁴The first PC in the Pacific has a shorter timescale than the first PC in the other regions, consistent with the weakened eddy feedbacks in a pulsed jet.

winds are switched on. We then assess the robustness in a series of equilibrium runs.

The meridional circulation associated with the QBO, as discussed in part 1, is manifested in the FBRANCH ensemble. In the first month after branching, zonally averaged NH temperature anomalies in the lowermost stratosphere resemble that shown in Part 1 (compare Figure 1 and 5 of part 1 to Figure 5b here). These temperature anomalies, and the associated upward and downward motion, are part of the circulation in thermal wind balance with the QBO. Zonal wind anomalies arch downward and poleward from the equatorial QBO anomaly, similar to the effect of the QBO in the absence of eddies (Figure 5a). Anomalies in the lowermost stratosphere in WACCM and in part 1 are nearly identical as the meridional circulation associated with the QBO in the absence of eddies is model independent. In the second month after branching, the lowermost stratospheric temperature anomalies are near their equilibrium values and the zonal wind horseshoe begins to extend into the troposphere (Figure 5c-d). In ensuing months, the horseshoe amplifies in the troposphere. NH anomalies in the fourth month after branching are quantitatively similar in WACCM and in the dry model (compare Figure 9 of part 1 to Figure 5f).

Figure 6 shows a map view of the response after branching with EQBO winds. Zonal wind anomalies at the 150hPa level are significant everywhere in the 15N-30N latitude band but are strongest in the Pacific near the jet exit region (Figure 6a,c,e). The meridional circulation associated with the QBO is stronger in the NH⁵. In the troposphere, the zonal wind anomalies develop more slowly, though in the fourth month after branching, the zonal wind anomaly in the North Pacific approaches 4m/s (Figure 6b,d,f). The westerly anomaly in the deep

⁵The asymmetry between hemispheres is much weaker in part 1 because the parametrizations for the troposphere are hemispherically symmetric.

Tropics, easterly anomaly in the subtropics, and westerly anomaly in the extratropics are strongest in the Pacific. The Atlantic and SH jet shifts poleward as well, consistent with expectations. These changes in the troposphere extend to the surface (not shown).

We now use the vorticity budget (Equation 1) to diagnose the contribution of transient eddies to the growth of tropospheric zonal wind anomalies and the associated vorticity anomalies in response to the QBO. In particular, we want to show the important role of vorticity fluxes by transient eddies for amplifying the vorticity anomalies and for extending them towards the surface. Figure 7 shows the anomalous vorticity forcing by high frequency eddies in the Pacific and Atlantic sectors four months after QBO winds are imposed in the FBRANCH ensemble. These eddy vorticity flux convergences strongly support the zonal wind anomalies shown in Figures 5 and 6. High frequency eddy forcing increases steadily after QBO onset, implying that eddy feedbacks are amplifying with the tropospheric response to the QBO. High frequency eddies in the Atlantic and Pacific are independent of each other and are not well correlated in time, but they react similarly to the external QBO forcing. In the reanalysis data as well, the difference in the high frequency eddy forcing between EQBO and WQBO reinforces the tropospheric NP zonal wind and vorticity anomalies (not shown, but like in Figure 7). Analysis of the stretching and wave terms in Equation 1 indicate that they are less important than the transient eddy flux, but do act to move vorticity anomalies downward and sustain them against surface drag (not shown), much as shown by BH10 for the NAO. Analysis of the vertical terms in Equation 1 indicate that they are important in the lowermost stratosphere but not below 200hPa. Like in Part 1, high frequency eddies are vital for amplifying the QBO signal in the troposphere.

a. Influence of Convection and Polar Vortex Variability

One might posit that the influence of the QBO on the polar vortex or on convection is involved in the QBO response in the troposphere. Even though part 1 found that high frequency eddies modify the jets in the troposphere even in the absence of convection and polar vortex variability, it is conceivable that these pathways are important in the atmosphere. We therefore investigate whether convection or polar vortex variability are important for the tropospheric response in FBRANCH.

We first discuss how convection changes over the course of the 120 days after branching. We then seek to understand how convective variability and polar vortex variability influence the NP in the FCONT run. Finally, we project the changes in convection and in the polar vortex in the FBRANCH ensemble onto the effect that such an anomaly had in FCONT. We can thus deduce the role that convection and polar vortex variability may have had in the FBRANCH ensemble.

Static stability is decreased, upward motion enhanced, and tropopause height increased, in the equatorial upper troposphere as part of the meridional circulation in thermal wind balance with EQBO winds (see Figure 5b, Section 4 of part 1, and Collimore et al. (2003)). These changes are expected to increase the height to which deep convection can rise in deep convecting regions of the Tropics, though it is not clear whether the amount of convection should be increased. To demonstrate that deep convecting cloud top heights are affected by the QBO, we show the change in outgoing longwave radiation(OLR) at the top of the atmosphere in the FBRANCH ensemble in Figure 8a,c,e. EQBO leads to a significant decrease in OLR where high clouds are present climatologically. The negative OLR anomalies

peak near Indonesia and Africa at 12.7Wm^{-2} in the first month and 23Wm^{-2} in the fourth month. Positive OLR anomalies are present in the subtropics and extratropics, consistent with the descending motion that is part of the meridional circulation of the QBO (Collimore et al. 2003). High cloud fraction is also enhanced fairly uniformly throughout the deep Tropics and decreased in the subtropics(not shown). The height to which deep convection can rise is affected by the QBO in the FBRANCH ensemble; it is likely that the QBO can influence the height to which deep convection can rise in the atmosphere as well.

Changes in OLR are well correlated with changes in total convection, but decreased OLR does not prove that there is more convection. We therefore examine convective mass flux, heating from moist processes, and total convective precipitation, to determine whether the total amount of tropical convection is modulated by the QBO. Zonally averaged convective mass flux and heating from moist processes are increased significantly at the 95% level equatorward of 6° above 400hPa, but in the lower troposphere, the change is no longer robust. Even at upper levels, the changes are highly zonally asymmetric. The strongest enhancement in convection is in the inter-tropical convergence zone (ITCZ) in the Pacific (e.g. convective precipitation in Figure 8). If the convection in the Pacific ITCZ is removed from the zonal average, the increase in the amount of tropical convection is no longer significant. Future work is necessary to understand why anomalies in the amount of convection are more regional than changes in OLR.

We now address whether variability in convection might cause the zonal wind anomalies in the extratropics in FBRANCH. We do this by first quantifying(in a linear sense) the connection between OLR variability and zonal wind variability in the FCONT run, and then applying this linear connection to the observed OLR anomalies in the FBRANCH ensemble.

The procedure is as follows. (1) The OLR anomalies for the FCONT run are decomposed into EOFs. (2) Multiple regression is used to relate OLR EOFs to zonal wind anomalies in the FCONT run. (3) The EOFs are projected against the OLR anomaly in month four (Figure 8e). (4) These projection coefficients are multiplied by the map that connects OLR EOFs to zonal wind anomalies in the FCONT run, thus generating the zonal wind associated (in a linear sense) with the OLR anomalies in Figure 8⁶. Figure 9a shows that a decrease in tropical OLR is typically associated with an intensification of the subtropical jet. An increase in tropical heating typically leads to stronger subtropical jet in dry models (e.g. Section 6 of part 1) and in observations (e.g. in El Niño) as well. EQBO leads to a weakening of the subtropical jet in our model runs, contrary to what might be expected from the change in OLR. Anomalies in convection due to the meridional circulation of the QBO are therefore not responsible for the extratropical response. Rather, changes in convection might damp the extratropical response.

We now investigate the role of polar vortex variability in the tropospheric response to the QBO in FBRANCH. The polar cap temperature increases by $\sim 1.5\text{K}$ over the course of the 120 day FBRANCH simulation ⁷. Linear regression is used to estimate the zonal wind

⁶A second method was also examined. The area averaged pattern correlation was taken between the OLR anomalies in Figure 8 with the OLR anomalies in each month of the control run. The resultant time series is normalized and is then regressed against the zonal wind anomalies of the control run. The zonal wind pattern is qualitatively similar to that shown in Figure 9a. Results are also qualitatively similar if the OLR pattern in month 1 or 2 after branching is used. Results are also qualitatively similar if the convective precipitation anomalies are used.

⁷Polar cap temperature is defined as the area averaged temperature from 70N and poleward and 70hPa to 150hPa. The increase is nearly 3K from 20hPa to 50hPa. Changes in Rossby wave propagation and EP flux

anomalies in the troposphere associated with such a temperature increase. A time series of the polar cap temperature anomaly in each month of the FCONT run is created, and the polar cap time series is then regressed against the zonal wind anomalies in the troposphere. Figure 9b shows the zonal wind anomalies associated with a 1.5K increase in polar cap temperature. The modulation of the troposphere by the vortex does not project onto the NP response to the QBO, just like in Garfinkel and Hartmann (2010). The vortex pathway is especially strong in the Atlantic where a weakened vortex leads to an equatorward shift in the jet, but even there the influence of the vortex on jet position is overwhelmed in our model run. We therefore conclude that the QBO is influencing high frequency eddies through its meridional circulation in thermal wind balance with the anomalous equatorial winds, like in the dry model in part 1 .

b. Robustness

The robustness of the FBRANCH results and the sensitivity to the choice of the date for the perpetual forcing are explored. We first discuss the JBRANCH ensemble before discussing the equilibrium EQBO cases.

Like in the FBRANCH ensemble, zonal wind anomalies in the JBRANCH ensemble extend out of the tropical stratosphere in a horseshoe pattern. The zonal wind anomaly at 150hPa is stronger in the Pacific sector of the Northern Hemisphere than in any other region (Figure 10). The zonal wind anomaly at 300hPa in the Pacific is qualitatively similar to,

convergence are broadly consistent with the Holton Tan mechanism; Garfinkel et al. (2011) will investigate the changes in Rossby wave propagation in more detail.

though much weaker than, the zonal wind anomaly in FBRANCH with 3x EQBO winds. The OLR anomalies are also qualitatively similar to those in the FBRANCH ensemble(not shown), but peak at only 4.5Wm^{-2} in the first month and 7Wm^{-2} in the third month after branching.

We now discuss the tropospheric response in the equilibrium EQBO runs (Figure 11-12).

- i. The subtropical jet in the NP in the perpetual January and February 3x EQBO equilibrium runs is significantly weaker than in the CONTROL cases, as expected(Figure 11a-b). The response is stronger in January than February, contrary to expectations⁸. The NP zonal wind anomaly in FBRANCH four months after branching is stronger in amplitude than the NP zonal wind anomaly in the equilibrium 3x EQBO run(Figure 11b vs. Figure 6f). Anomalies in OLR are near their equilibrium value by the fourth month after branching (Figure 12b vs. Figure 8f) as well, suggesting that the tropospheric response to QBO winds equilibrates after four months.
- ii. The response in the NP to the default EQBO profile qualitatively resembles the response to the 3x EQBO profile(Figure 11c-d and Figure 12c-d). The zonal wind anomaly in the NP in JBRANCH reaches the amplitude of that in the equilibrium EQBO run three months after branching (Figure 10 vs. Figure 11c).
- iii. Including upper stratospheric westerlies present in realistic QBO profiles weakens the zonal wind response in the NP(Figure 11e-f) and the tropical OLR response (Fig-

⁸In the strong subtropical jet case in Part 1a, the jet shifts equatorwards and not poleward in response to EQBO winds to maintain stability. Here, the jet is stable in all cases examined and shifts polewards. Nevertheless, a weaker shift is expected in January than in February because of weakened eddy feedback in January.

ure 12e-f), but the overall pattern is nearly identical. Sensitivity of the tropospheric response to upper stratospheric westerlies is weak. Such weak sensitivity might be expected from the nearly identical meridional circulations in the lower stratosphere between Figure 6a and 6h of Part 1.

- iv. The NP zonal wind response to weak EQBO winds forced only below the 0.061 hybrid σ level is comparable to the response when winds are relaxed over more of the stratosphere in perpetual February (Figure 11h vs. 11d) but not in perpetual January. The difference in NP zonal wind response between perpetual February and perpetual January is statistically significant, consistent with expectations. The OLR response is qualitatively similar, and is stronger in February than in January (Figure 12h vs. 12d).
- v. The response to weak EQBO winds forced only above the 0.061 hybrid σ level is significant only in the perpetual February case (Figure 11i-j and Figure 12i-j). The winds between 100hPa and 60hPa are similar to the control case, so that the thermal wind balanced meridional circulation associated with the QBO is weaker in the lowermost stratosphere (not shown). The NP zonal wind response is significantly stronger in February than in January, consistent with observations and the dry model in part 1. Changes in OLR in the deep convecting regions of the Tropics are smaller than that for the other QBO profiles tested, suggesting that the direct modulation of tropical convection is weaker when QBO wind anomalies do not extend into the lowermost stratosphere (Figure 12i-j). We therefore expect that a model whose internally generated QBO does not extend deeply enough into the lower stratosphere will miss some of the effect of the QBO in the troposphere.

Even though the response in these cases varies as the QBO winds relaxed towards vary, the NP responses, if present, are qualitatively similar. The similarity in response suggests that in all of these cases, the QBO affects the subtropical NP by influencing tropospheric eddies. Finally, we have examined the tropospheric response to realistic WQBO stratospheric winds and to 3x WQBO winds. The response to WQBO winds is nearly equal (though the magnitude of the anomalies is slightly weaker) and opposite to that for EQBO shown in Figure 11; details are excluded for brevity.

The effect of the QBO in the troposphere in the Atlantic is only robust with 3x EQBO winds. The weakened response to realistic EQBO winds is consistent with Part 1, where we found that only 3x EQBO winds affected a jet whose mean position is near 40° (J40 in Section 5). Furthermore, the effect of the QBO in the troposphere through the polar vortex is particularly strong in the Atlantic sector (e.g. Figure 9b) and opposes the affect of the QBO on tropospheric eddies through its thermal wind balanced meridional circulation. Finally, the modeled North Atlantic response to WQBO winds is not robust (not shown). The net effect of realistic QBO winds in the North Atlantic in January and February is weak, just like in the reanalysis and coupled seasonal WACCM run in Figure 1.

In the cases shown here, as well as in Figure 6f, the QBO appears to influence the SAM near Australia and the Indian Ocean. The SH tropospheric jet is shifted polewards in response to EQBO winds, consistent with expectations. While this seems to be a robust feature in WACCM, it does not appear in the reanalysis(e.g. Figure 1). As discussed in Section 3, the SH mean state in the FCONT and JCONT runs is not particularly true to the observed mean state. Only a seasonal integration of WACCM can accurately model the SH. We are therefore not ready to attach any meaning to a comparison of these SH WACCM

results to the reanalysis.

5. Conclusions

In this paper we have examined the tropospheric response to easterly QBO wind anomalies using an ensemble of experiments with the WACCM. The results support previous work done with a dry model in Part 1.

In both the reanalysis record and in a coupled seasonal WACCM run, winds are significantly weaker near and south of the climatological jet position in the subtropical Pacific during the easterly phase of the QBO relative to its westerly phase in February and March. To understand why the QBO may have the influence it appears to have, the influence of the QBO on the troposphere in perpetual February and January WACCM runs with fixed SSTs is studied. As shown in part 1, QBO momentum anomalies require a meridional circulation to establish thermal wind balance. The zonal wind associated with this circulation arches down to the subtropical troposphere.

In the presence of eddies, the subtropical Pacific jet is weakened and contracted, and the response is stronger in February than in January. High frequency eddies are important for the response in the troposphere. All of these responses are similar to those found for a dry GCM in part 1. Cloud tops rise in response to the QBO, likely in response to the circulation that brings the easterly stratospheric wind anomalies into geostrophic balance. But these convective anomalies appear to work against the extratropical tropospheric circulation anomalies. Qualitative resemblance between the anomalies shown here and in the reanalysis suggests that our model can capture the mechanisms through which the QBO influences the

troposphere.

Garfinkel and Hartmann (2010) argue that the QBO influences El Niño teleconnections. The results here and in part 1 affirm (1) that the QBO can alter the background state in the North Pacific experienced by an anomalous Rossby wavetrain as it propagates poleward away from anomalous SSTs and (2) that the “direct” effect in Section 4 of Garfinkel and Hartmann (2010) is a real physical phenomenon.

The response to the QBO is strongest in the North Pacific in February and weaker in other basins and in January, consistent with Part 1 and observations. Our results highlight the sensitivity of the response to the mean state of the unperturbed climate. We therefore strongly suggest that when studying the tropospheric response to other external perturbations, attention should be paid to regional and intra-seasonal differences.

The perpetual January and February model runs used here still have limitations in their ability to simulate the actual atmosphere. In our model runs, the stratospheric QBO winds do not propagate downwards but rather remain fixed. Because the lowermost stratospheric meridional circulation has reached most of its strength by the second month, we expect that the stratospheric circulation for a downwards propagating QBO will be nearly identical to that shown here and in part 1. The tropospheric anomalies do not reach their equilibrium value until the third or fourth month after branching; we therefore expect a slightly weaker tropospheric response for a downwards propagating QBO than that shown here. Our methodology also precludes a meaningful analysis of beating of the QBO with the annual cycle or of decadal variability (Ruzmaikin et al. 2005; Lu et al. 2008). The QBO in our model configuration is imposed by relaxing towards a specified tropical zonal wind profile. Attempts to incorporate an internally generated QBO into GCMs have met with increasing

success. Many of these models still have trouble simulating the propagation of QBO anomalies down to the lowermost stratosphere, however. The current generation of models that internally generate a QBO may therefore have difficulty capturing the effect of the QBO in the troposphere. Should the internally generated QBO winds in future generations of models reach the lowermost stratosphere, it will be attractive to use such models to revisit the QBO's affect on the troposphere. Finally, models with a more realistic sudden stratospheric warming frequency and with better resolved convection are necessary to confirm our results. Nevertheless, similarity among our perpetual winter WACCM and dry model runs, the fully coupled seasonal WACCM run, and the reanalysis suggest that the mechanism we are describing is real and robust.

Results presented here, in Dall'Amico et al. (2010), in Giorgetta et al. (1999), and in Marshall and Scaife (2009), suggest that seasonal forecasting of tropospheric variability could be improved as QBO phase is predictable months in advance. In particular, the current generation of models should incorporate zonal mean zonal wind relaxation to predicted QBO-dependent anomalous winds.

Acknowledgments.

This work was supported by the National Science Foundation under grant AGS 0960497. We thank the developers at NCAR for the WACCM 3.1.9, Elizabeth Barnes for providing the terms of the vorticity budget for the reanalysis, our anonymous reviewers for their helpful comments, and Marc L. Michelsen for assisting our model runs.

REFERENCES

- Anstey, J. A., T. G. Shepherd, and J. F. Scinocca, 2010: Influence of the quasi-biennial oscillation on the extratropical winter stratosphere in an atmospheric general circulation model and in reanalysis data. *J. Atmos. Sci.*, **67**, 1402–1419, doi:10.1175/2009JAS3292.1.
- Baldwin, M. P. and T. J. Dunkerton, 1999: Propagation of the Arctic Oscillation from the stratosphere to the troposphere. *J. Geophys. Res.*, **104 (D24)**, 30 937–30 946.
- Baldwin, M. P., et al., 2001: The Quasi-Biennial Oscillation. *Rev. Geophys.*, **39 (2)**, 179–229.
- Barnes, E. and D. Hartmann, 2010a: Dynamical feedbacks and the persistence of the nao. *J. Atmos. Sci.*, **67**, 851–865, doi:10.1175/2009JAS3193.1.
- Barnes, E. and D. Hartmann, 2010b: Dynamical feedbacks of the southern annular mode in winter and summer. *J. Atmos. Sci.*, **67**, 2320–2330, doi:10.1175/2010JAS3385.1.
- Barnes, E. A., D. L. Hartmann, D. M. W. Frierson, and J. Kidston, 2010: Effect of latitude on the persistence of eddy-driven jets. *Geophys. Res. Lett.*, **37 (L11804)**, 2320–2330, doi:10.1029/2010GL043199.
- Collimore, C. C., D. W. Martin, M. H. Hitchman, A. Huesmann, and D. E. Waliser, 2003: On the relationship between the QBO and tropical deep convection. *J. Clim.*, **16 (15)**, doi:10.1175/1520-0442(2003).

- Collins, W. D., et al., 2006: The Formulation and Atmospheric Simulation of the Community Atmosphere Model Version 3 (CAM3). *Journal of Climate*, **19**, doi:10.1175/JCLI3760.1.
- Coughlin, K. and K.-K. Tung, 2001: QBO Signal found at the Extratropical Surface through Northern Annular Modes. *Geophys. Res. Lett.*, **28**, 4563–4566, doi:10.1029/2001GL013565.
- Coughlin, K. T. and K. K. Tung, 2005: Empirical mode decomposition of climate variability in the atmospheric. *Hilbert-Huang Transform: Introduction and Application*, N. Huang and S. Shen, Eds., World Scientific Publishing, 149–164.
- Crooks, S. A. and L. J. Gray, 2005: Characterization of the 11-year solar signal using a multiple regression analysis of the ERA-40 dataset. *J. Clim.*, **18**, 996–1015.
- Dall’Amico, M., P. A. Stott, A. A. Scaife, L. J. Gray, K. H. Rosenlof, and A. Y. Karpechko, 2010: Impact of stratospheric variability on tropospheric climate change. *Climate Dynamics*, **34**, 399–417, doi:10.1007/s00382-009-0580-1.
- Eichelberger, S. J. and D. L. Hartmann, 2007: Zonal jet structure and the leading mode of variability. *J. Clim.*, **20**, doi:10.1175/JCLI4279.1.
- Garcia, R. R., D. Marsh, D. Kinnison, B. Boville, and F. Sassi, 2007: Simulations of secular trends in the middle atmosphere, 1950-2003. *J. Geophys. Res.*, **112**, D09301, doi:10.1029/2006JD007485.
- Garfinkel, C. I. and D. L. Hartmann, 2007: Effects of the El-Nino Southern Oscillation and the Quasi-Biennial Oscillation on polar temperatures in the stratosphere. *J. Geophys. Res.- Atmos.*, **112**, D19112, doi:10.1029/2007JD008481.

- Garfinkel, C. I. and D. L. Hartmann, 2010: The influence of the quasi-biennial oscillation on the north pacific and el-niño teleconnections. *J. Geophys. Res.*, **115**, D20116, doi:10.1029/2010JD014181.
- Garfinkel, C. I. and D. L. Hartmann, 2011: The influence of the Quasi-Biennial Oscillation on the troposphere in wintertime in a hierarchy of models, part 1-simplified dry GCMs. *J. Atmos. Sci.*, **submitted**.
- Garfinkel, C. I., T. A. Shaw, D. L. Hartmann, and D. W. Waugh, 2011: The influence of the quasi-biennial oscillation on the arctic polar vortex in perpetual winter waccm runs. *J. Atmos. Sci.*, **in preparation**.
- Gerber, E. P. and L. M. Polvani, 2009: Stratosphere-troposphere coupling in a relatively simple agcm: The importance of stratospheric variability. *J. Clim.*, **22**, 1920–1933, doi:10.1175/2008JCLI2548.1.
- Giorgetta, M. A., L. Bengtsson, and K. Arpe, 1999: An investigation of QBO signals in the east Asian and Indian monsoon in GCM experiments. *Climate Dynamics*, **15**, 435–450, doi:10.1007/s003820050292.
- Giorgetta, M. A., E. Manzini, E. Roeckner, M. Esch, and L. Bengtsson, 2006: Climatology and Forcing of the Quasi-Biennial Oscillation in the MAECHAM5 Model. *Journal of Climate*, **19**, 3882–+, doi:10.1175/JCLI3830.1.
- Haigh, J. D., M. Blackburn, and R. Day, 2005: The response of tropospheric circulation to perturbations in lower-stratospheric temperature. *J. Clim.*, **18**, 3672–3685, doi:10.1175/JCLI3472.1.

- Ho, C., H. Kim, J. Jeong, and S. Son, 2009: Influence of stratospheric quasi-biennial oscillation on tropical cyclone tracks in the western North Pacific. *Geophys. Res. Lett.*, **36**, doi:10.1029/2009GL037163.
- Holton, J. R. and H. C. Tan, 1980: The influence of the equatorial Quasi-Biennial Oscillation on the global circulation at 50mb. *J. Atmos. Sci.*, **37**, 2200–2208.
- Huesmann, A. S. and M. H. Hitchman, 2001: The stratospheric quasi-biennial oscillation in the NCEP reanalyses: Climatological structures. *J. Geophys. Res.*, **106**, 11 859–11 874, doi:10.1029/2001JD900031.
- Kawatani, Y., S. Watanabe, K. Sato, T. J. Dunkerton, S. Miyahara, and M. Takahashi, 2010: The roles of equatorial trapped waves and internal inertia – gravity waves in driving the quasi-biennial oscillation. part i: Zonal mean wave forcing. *Journal of Atmospheric Sciences*, **67**, 963–980, doi:10.1175/2009JAS3222.1.
- Kulyamin, D. V., E. M. Volodin, and V. P. Dymnikov, 2009: Simulation of the quasi-biennial oscillations of the zonal wind in the equatorial stratosphere: Part ii. atmospheric general circulation models. *Izvestiya Atmospheric and Oceanic Physics*, **45**, 37–54, doi: 10.1134/S0001433809010046.
- Limpasuvan, V., D. W. J. Thompson, and D. L. Hartmann, 2004: The life cycle of the Northern Hemisphere sudden stratospheric warmings. *J. Clim.*, **17**, 2584–2596.
- Lorenz, D. J. and D. L. Hartmann, 2001: Eddy-zonal flow feedback in the southern hemisphere. *J. Atmos. Sci.*, **58**, 3312–3326.

- Lu, H., M. P. Baldwin, L. J. Gray, and M. J. Jarvis, 2008: Decadal-scale changes in the effect of the QBO on the northern stratospheric polar vortex. *Journal of Geophysical Research (Atmospheres)*, **113**, 10 114–+, doi:10.1029/2007JD009647.
- Marsh, D., R. R. Garcia, D. E. Kinnison, B. A. Boville, F. Sassi, S. C. Solomon, and K. Matthes, 2007: Modeling the whole atmosphere response to solar cycle changes in radiative and geomagnetic forcing. *J. Geophys. Res.*, **112**, doi:10.1029/2006JD008306.
- Marshall, A. G. and A. A. Scaife, 2009: Impact of the QBO on surface winter climate. *Journal of Geophysical Research (Atmospheres)*, **114**, 18 110–+, doi:10.1029/2009JD011737.
- Matthes, K., D. R. Marsh, R. R. Garcia, D. E. Kinnison, F. Sassi, and S. Walters, 2010: Role of the QBO in modulating the influence of the 11 year solar cycle on the atmosphere using constant forcings. *J. Geophys. Res.*, **115**, D18 110, doi:10.1029/2009JD013020.
- Osprey, S. M., L. J. Gray, S. C. Hardiman, N. Butchart, A. C. Bushell, and T. J. Hinton, 2010: The climatology of the middle atmosphere in a vertically extended version of the met office’s climate model. part ii: Variability. *J. Atmos. Sci.*, **67**, doi:10.1175/2010JAS3338.1.
- Polvani, L. M. and P. J. Kushner, 2002: Tropospheric response to stratospheric perturbations in a relatively simple general circulation model. *Geophys. Res. Lett.*, **29**, doi:10.129/2001GL014284.
- Ruzmaikin, A., J. Feynman, X. Jiang, and Y. L. Yung, 2005: Extratropical signature of the Quasi-Biennial Oscillation. *J. Geophys. Res.*, **110**, D1111, doi:10.1029/2004JD005382.
- Uppala, S. M., et al., 2005: The ERA-40 reanalysis. *Quart. J. Roy. Meteorol. Soc.*

Zhang, G. J. and N. A. McFarlane, 1995: Sensitivity of climate simulations to the parameterization of cumulus convection in the canadian climate centre general circulation model. *Atmospheres and Oceans*, **33**, 407–446.

List of Tables

- 1 Different runs for understanding the tropospheric signal of the QBO. For the branch runs, the first number of “run length” denotes the number of ensemble members, each of which extend for 4 months. For all other runs, the run length denotes the number of months. 33
- 2 Characteristics of the first and second principal component of daily 925hPa zonal wind variability in the North Atlantic(60W-0W,20N and poleward), North Pacific(150E-150W,20N and poleward), and Southern Hemisphere(20S and poleward). Each cell contains, in order, the persistence timescale (in days) for the first EOF, the percentage of variance explained by the first EOF, the persistence timescale (in days) for the second EOF, and the percentage of variance explained by the second EOF. In JCONT and FCONT, the first EOF of SH and North Atlantic variability resemble a shifting jet. 34

Different runs of WACCM for QBO influence on Troposphere

	Month	QBO profile	run length
JCONT	Jan	QBOclim	463
FCONT	Feb	QBOclim	225
JBRANCH	Jan	EQBO	168x4
FBRANCH	Feb	3x EQBO	68x4
JEquil1	Jan	3x EQBO	219
FEquil1	Feb	3x EQBO	182
JEquil2	Jan	EQBO	168
FEquil2	Feb	EQBO	167
JEquil3	Jan	EQBOupperwest	278
FEquil3	Feb	EQBOupperwest	181
JEquil4	Jan	EQBO6090	167
FEquil4	Feb	EQBO6090	152
JEquil5	Jan	EQBOtop	167
FEquil5	Feb	EQBOtop	171

TABLE 1. Different runs for understanding the tropospheric signal of the QBO. For the branch runs, the first number of “run length” denotes the number of ensemble members, each of which extend for 4 months. For all other runs, the run length denotes the number of months.

Timescale and Variance explained for the First Two EOFs

	NAtlantic	NPacific	SH
JCONT	14.6, 29.8±1.5%, 6.7, 15.1±0.5%	13.6, 23.5±1.2%, 11.7, 15.5±0.7%	26.9, 9.2±0.6%, 6.5, 4.7±0.2%
FCONT	23.5, 32.7±2.7%, 6.2, 14.2±0.6%	14.3, 22.2±1.4%, 12.4, 16.2±1.0%	48.1, 8.3±1.0%, 5.0, 3.7±0.1%

TABLE 2. Characteristics of the first and second principal component of daily 925hPa zonal wind variability in the North Atlantic(60W-0W,20N and poleward), North Pacific(150E-150W,20N and poleward), and Southern Hemisphere(20S and poleward). Each cell contains, in order, the persistence timescale (in days) for the first EOF, the percentage of variance explained by the first EOF, the persistence timescale (in days) for the second EOF, and the percentage of variance explained by the second EOF. In JCONT and FCONT, the first EOF of SH and North Atlantic variability resemble a shifting jet.

List of Figures

- 1 Zonal wind anomalies at 300hPa associated with the QBO(EQBO-WQBO) in February and March in the ECMWF reanalysis data and a coupled seasonal WACCM run. See Section 2 of Part 1 for a description of the two data sources. Months with the wind anomalies at 70hPa exceeding 2m/s are used to define composites of EQBO and WQBO. There are 45 WQBO months and 30 EQBO months in the reanalysis composites, and 101 WQBO months and 73 EQBO months in the WACCM composites. Contours shown at $\pm 0.5, \pm 1.5, \pm 3, \pm 5, \pm 8$ m/s. Significant regions at 95% are shaded and negative contours are bolded. 38
- 2 The QBO profiles relaxed towards in the WACCM runs. Stars represent the 5% – 95% range of variability of equatorial zonal wind from May 1953 to April 2007. 39
- 3 Average zonal mean zonal wind and temperature in the reanalysis in January and in the JCONT run. Contours shown at $\pm 5, \pm 15, \pm 25, \pm 35, \pm 45, \pm 55, \pm 65$ m/s and every 10K. Shading marks regions where the mean state in February (FCONT) differs from that in January (JCONT) by 1K or 2m/s. 40
- 4 Time average zonal wind (shading and stars) and first two EOFs of 925hPa zonal wind(countours), in the JCONT and FCONT run. Contours shown at $\pm 1, \pm 2, \pm 3, \pm 4, \pm 5, \pm 6, \pm 7$ m/s at 925hPa. Shading marks regions where the mean wind exceeds ± 5 m/s at 925hPa (the lower level Pacific jet is less zonally asymmetric than the upper level Pacific jet). Stars mark the jet maximum. 41

- 5 Zonally averaged zonal wind and temperature anomalies one, two, and fourth months after branching in the perpetual February ensemble with a 3x EQBO profile (i.e. FBRANCH). Contours shown at $\pm 0.33, \pm 1, \pm 2, \pm 5, \pm 10, \pm 20$ m/s and $\pm 0.25, \pm 0.75, \pm 1.5, \pm 3, \pm 6$ K. The plotting conventions from part 1 are used to ease comparison. Significant regions at 95% are shaded and negative contours are bolded. 42
- 6 Zonal wind anomalies after branching in the perpetual February ensemble with a 3x EQBO profile (i.e. FBRANCH). Contour shown at $\pm 0.5, \pm 1.5, \pm 3, \pm 5, \pm 8$ m/s. Significant regions at 95% are shaded and negative(easterly) contours are bolded. The response in the third month after branching is omitted for brevity. 43
- 7 Contours denote anomalous upper level (i.e. 300hPa to 150hPa) high frequency eddy term of the vorticity budget in the fourth month after branching in the FBRANCH ensemble. Contour interval is $1.5 \cdot 10^{-12} s^{-2}$. Shading denotes mass weighted vorticity anomalies between 700hPa to 925hPa that exceed $1.75 \times 10^{-6} s^{-1}$. 44
- 8 OLR at the top of the atmosphere and convective precipitation anomalies after branching for the 3x EQBO ensemble in perpetual February (i.e. FBRANCH). Contours shown at $\pm 3, \pm 9, \pm 15, \pm 21, \text{ and } \pm 27$ W/m^{-2} for OLR, and $\pm 0.1, \pm 0.3, \pm 0.5, \pm 0.7,$ and ± 0.9 $mm \text{ day}^{-1}$ for convective precipitation. Significant regions at 95% are shaded and negative contours are bolded. 45

- 9 Zonal wind anomalies linearly associated with the OLR anomalies in month 4 of Figure 8 and with the weakening of the polar vortex for the FBRANCH ensemble. Contours shown at $\pm 0.5, \pm 1.5, \pm 3, \pm 5, \pm 8$ m/s. Regions with large anomalies are shaded. 46
- 10 Like Figure 6 but for the perpetual January ensemble with the default EQBO profile (i.e. JBRANCH). 47
- 11 Difference in zonal wind between the equilibrium EQBO cases and the FCONT and JCONT control cases for the different EQBO wind profiles. Below each panel is the difference in polar cap temperature (area averaged 70N and poleward from 70hPa to 150hPa) between each control case and the EQBO case. Contour interval like that in Figure 6. Significant regions at 95% are shaded and negative(easterly) contours are bolded. 48
- 12 Like Figure 11 but for OLR. Contour interval like that in Figure 8. 49

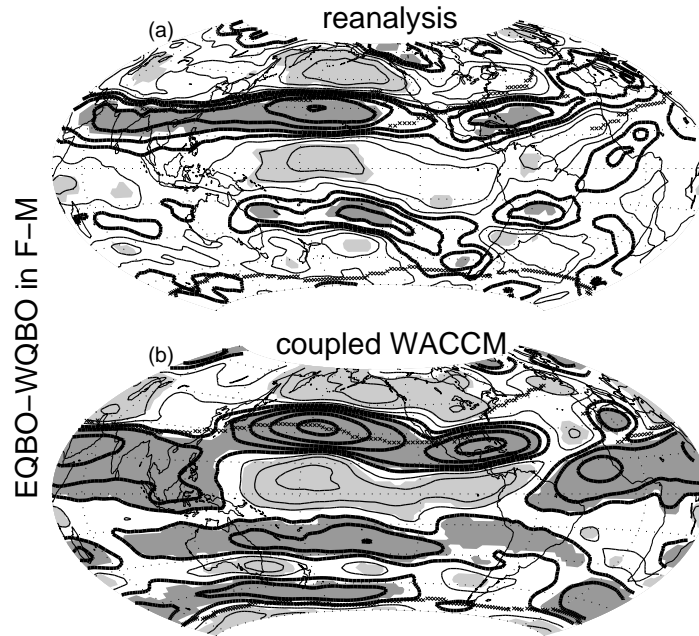


FIG. 1. Zonal wind anomalies at 300hPa associated with the QBO(EQBO-WQBO) in February and March in the ECMWF reanalysis data and a coupled seasonal WACCM run. See Section 2 of Part 1 for a description of the two data sources. Months with the wind anomalies at 70hPa exceeding 2m/s are used to define composites of EQBO and WQBO. There are 45 WQBO months and 30 EQBO months in the reanalysis composites, and 101 WQBO months and 73 EQBO months in the WACCM composites. Contours shown at $\pm 0.5, \pm 1.5, \pm 3, \pm 5, \pm 8$ m/s. Significant regions at 95% are shaded and negative contours are bolded.

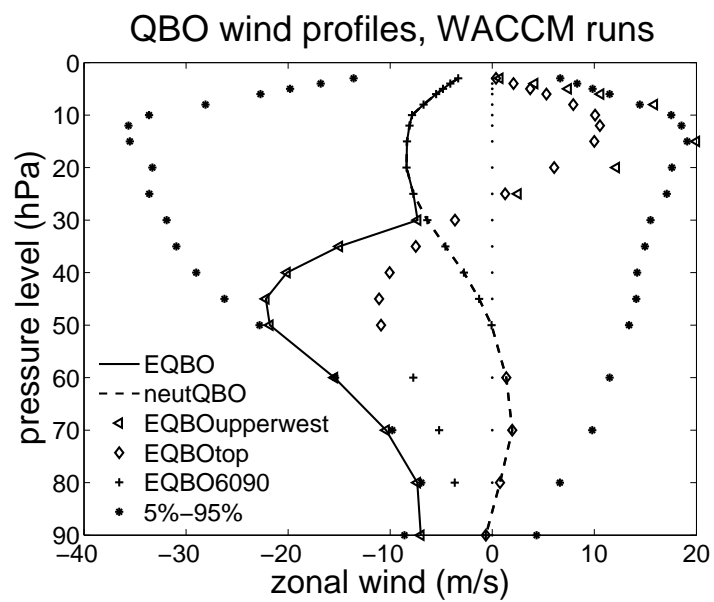


FIG. 2. The QBO profiles relaxed towards in the WACCM runs. Stars represent the 5%–95% range of variability of equatorial zonal wind from May 1953 to April 2007.

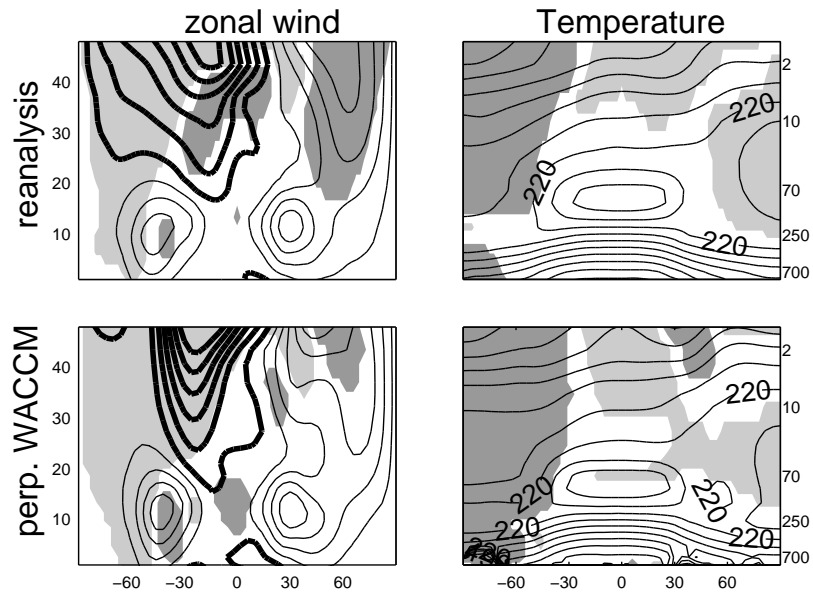


FIG. 3. Average zonal mean zonal wind and temperature in the reanalysis in January and in the JCONT run. Contours shown at $\pm 5, \pm 15, \pm 25, \pm 35, \pm 45, \pm 55, \pm 65$ m/s and every 10K. Shading marks regions where the mean state in February (FCONT) differs from that in January (JCONT) by 1K or 2m/s.

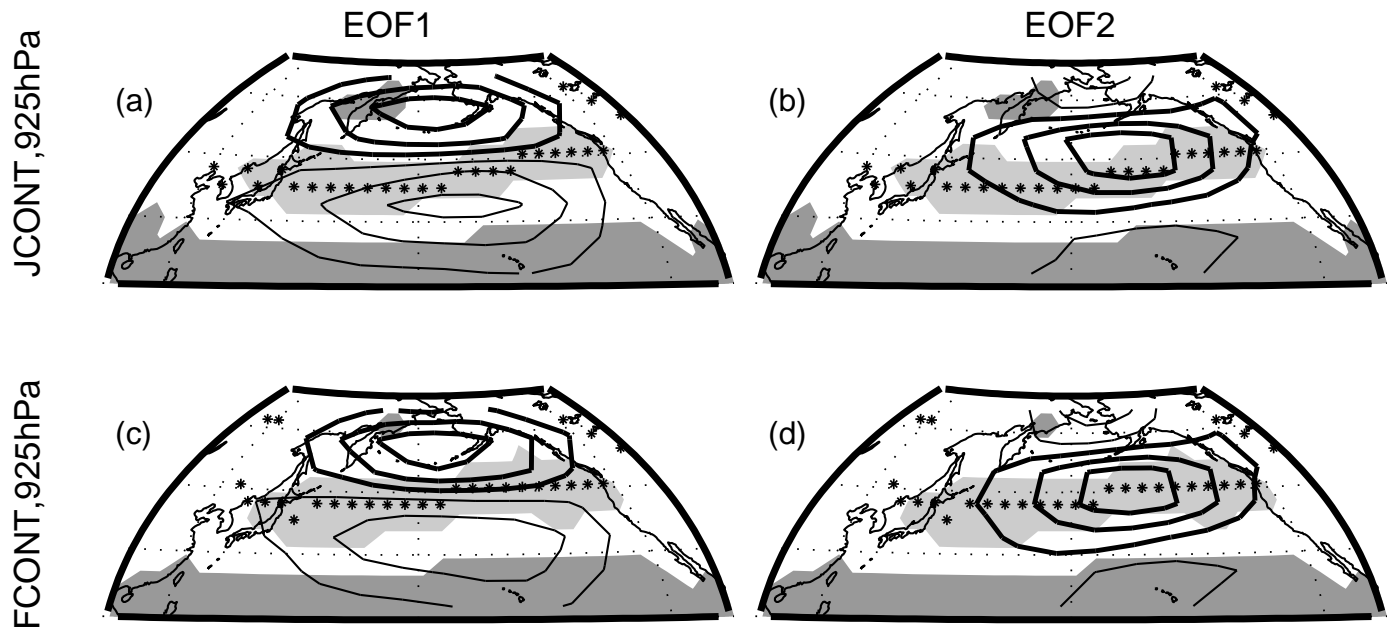


FIG. 4. Time average zonal wind (shading and stars) and first two EOFs of 925hPa zonal wind (contours), in the JCONT and FCONT run. Contours shown at $\pm 1, \pm 2, \pm 3, \pm 4, \pm 5, \pm 6, \pm 7$ m/s at 925hPa. Shading marks regions where the mean wind exceeds ± 5 m/s at 925hPa (the lower level Pacific jet is less zonally asymmetric than the upper level Pacific jet). Stars mark the jet maximum.

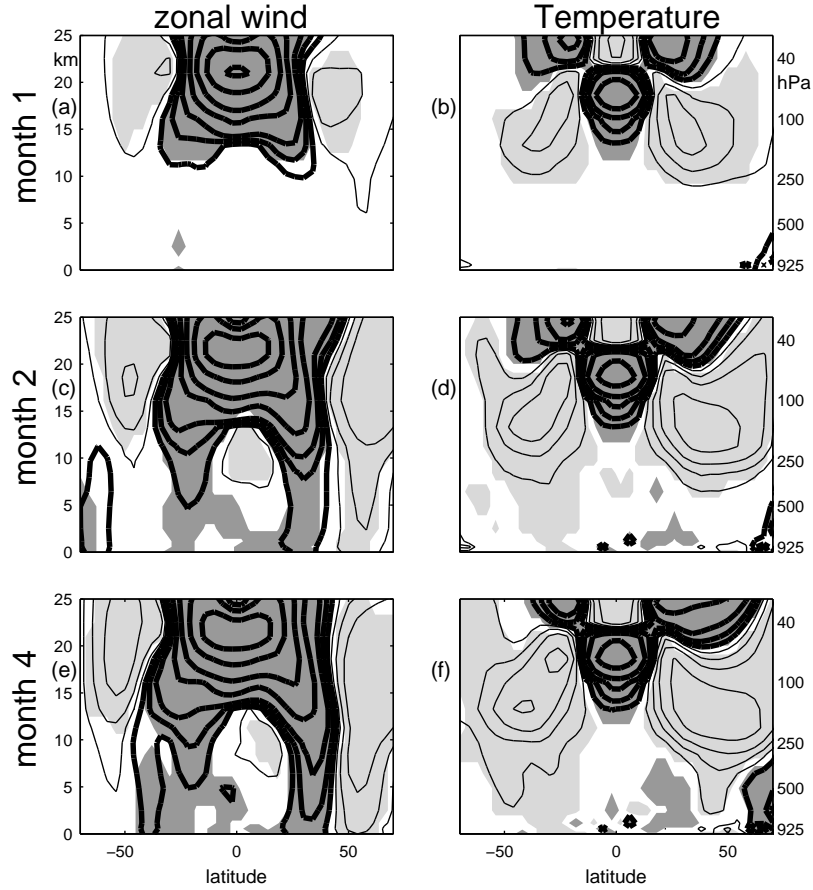


FIG. 5. Zonally averaged zonal wind and temperature anomalies one, two, and fourth months after branching in the perpetual February ensemble with a 3x EQBO profile (i.e. FBRANCH). Contours shown at $\pm 0.33, \pm 1, \pm 2, \pm 5, \pm 10, \pm 20$ m/s and $\pm 0.25, \pm 0.75, \pm 1.5, \pm 3, \pm 6$ K. The plotting conventions from part 1 are used to ease comparison. Significant regions at 95% are shaded and negative contours are bolded.

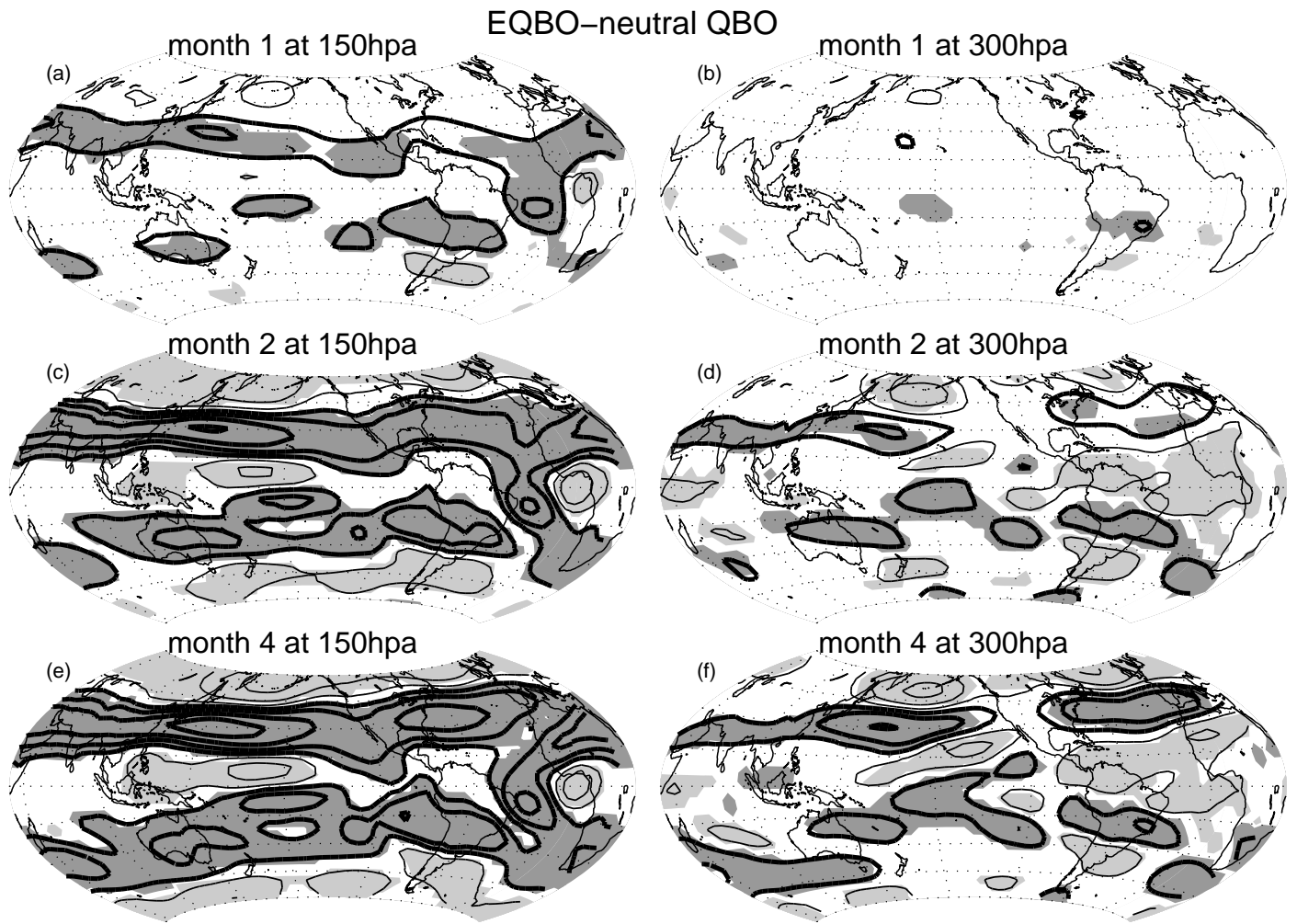


FIG. 6. Zonal wind anomalies after branching in the perpetual February ensemble with a 3x EQBO profile (i.e. FBRANCH). Contour shown at $\pm 0.5, \pm 1.5, \pm 3, \pm 5, \pm 8$ m/s. Significant regions at 95% are shaded and negative (easterly) contours are bolded. The response in the third month after branching is omitted for brevity.

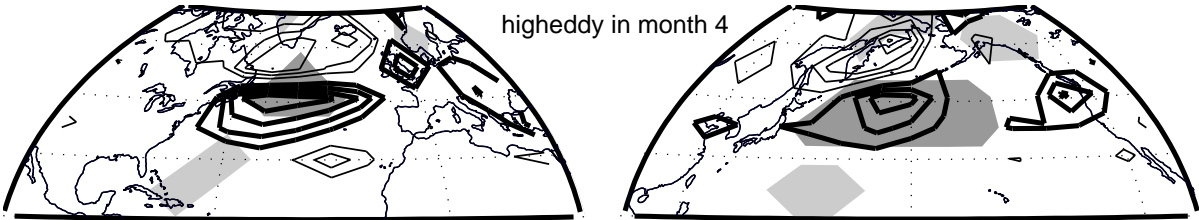


FIG. 7. Contours denote anomalous upper level (i.e. 300hPa to 150hPa) high frequency eddy term of the vorticity budget in the fourth month after branching in the FBRANCH ensemble. Contour interval is $1.5 \cdot 10^{-12} s^{-2}$. Shading denotes mass weighted vorticity anomalies between 700hPa to 925hPa that exceed $1.75 \times 10^{-6} s^{-1}$.

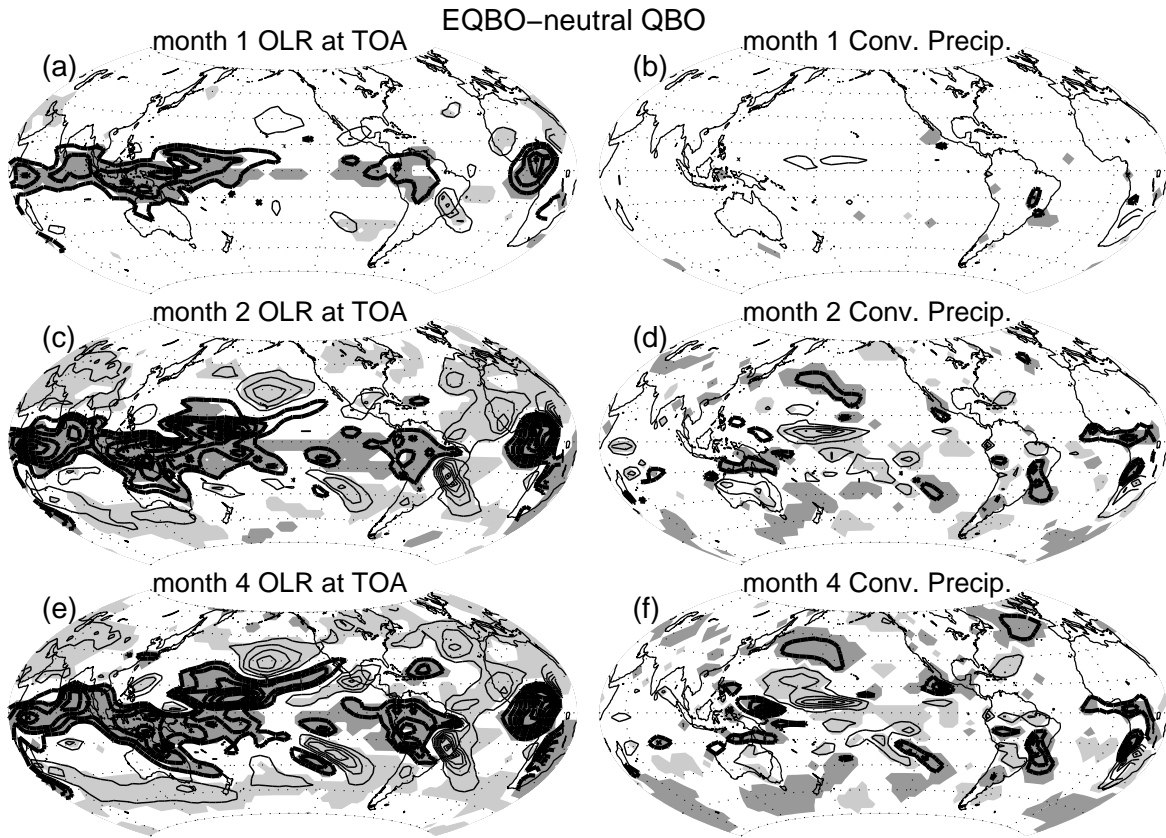


FIG. 8. OLR at the top of the atmosphere and convective precipitation anomalies after branching for the 3x EQBO ensemble in perpetual February (i.e. FBRANCH). Contours shown at $\pm 3, \pm 9, \pm 15, \pm 21,$ and $\pm 27 \text{ W/m}^{-2}$ for OLR, and $\pm 0.1, \pm 0.3, \pm 0.5, \pm 0.7,$ and $\pm 0.9 \text{ mm day}^{-1}$ for convective precipitation. Significant regions at 95% are shaded and negative contours are bolded.

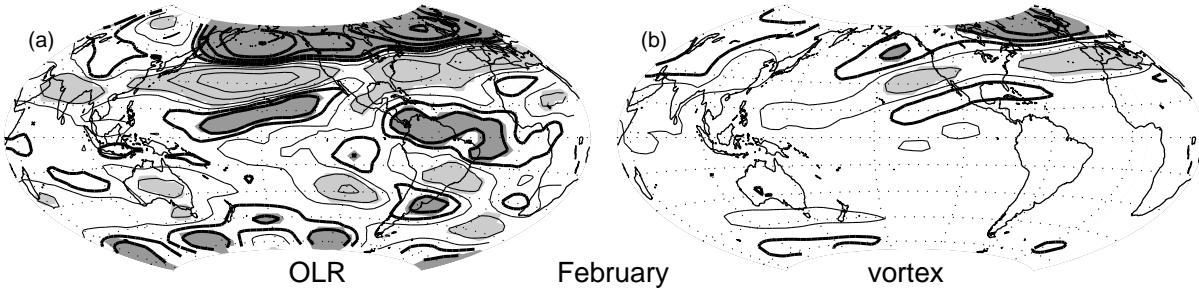


FIG. 9. Zonal wind anomalies linearly associated with the OLR anomalies in month 4 of Figure 8 and with the weakening of the polar vortex for the FBRANCH ensemble. Contours shown at ± 0.5 , ± 1.5 , ± 3 , ± 5 , ± 8 m/s. Regions with large anomalies are shaded.

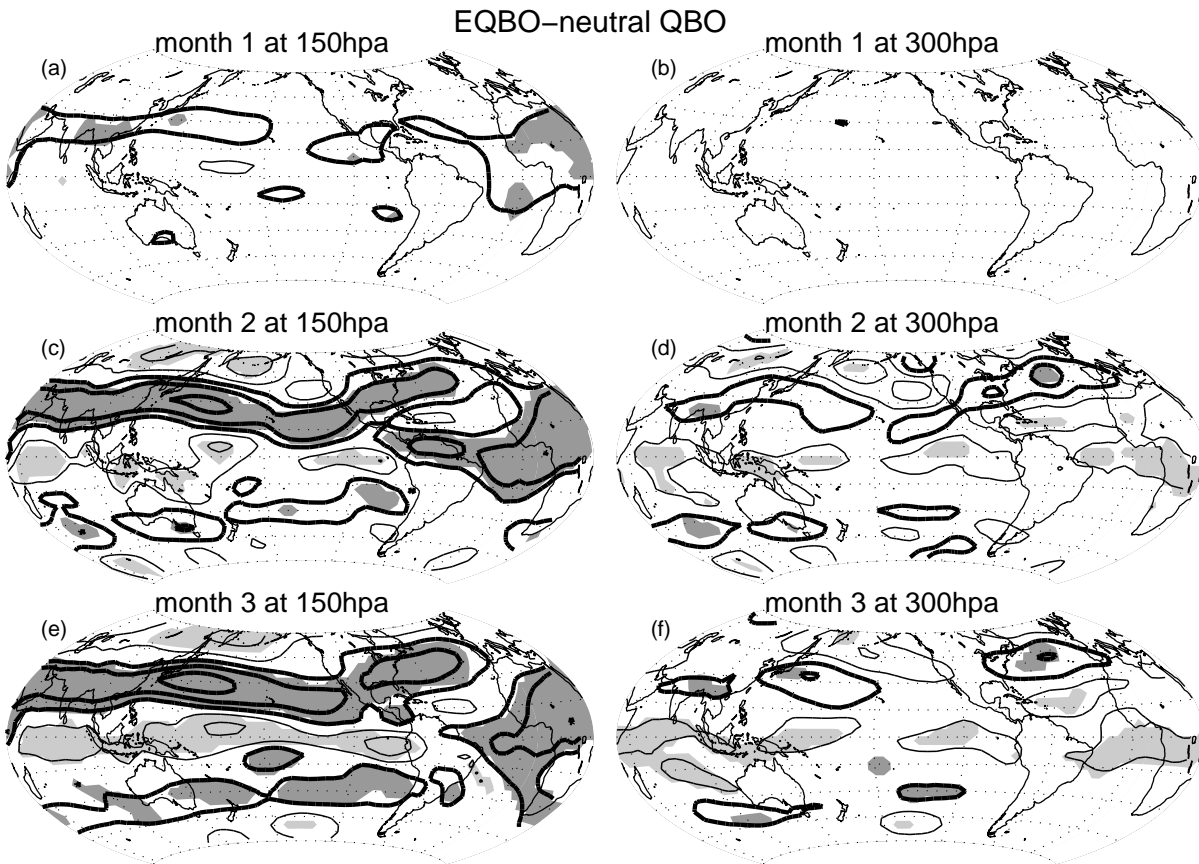


FIG. 10. Like Figure 6 but for the perpetual January ensemble with the default EQBO profile (i.e. JBRANCH).

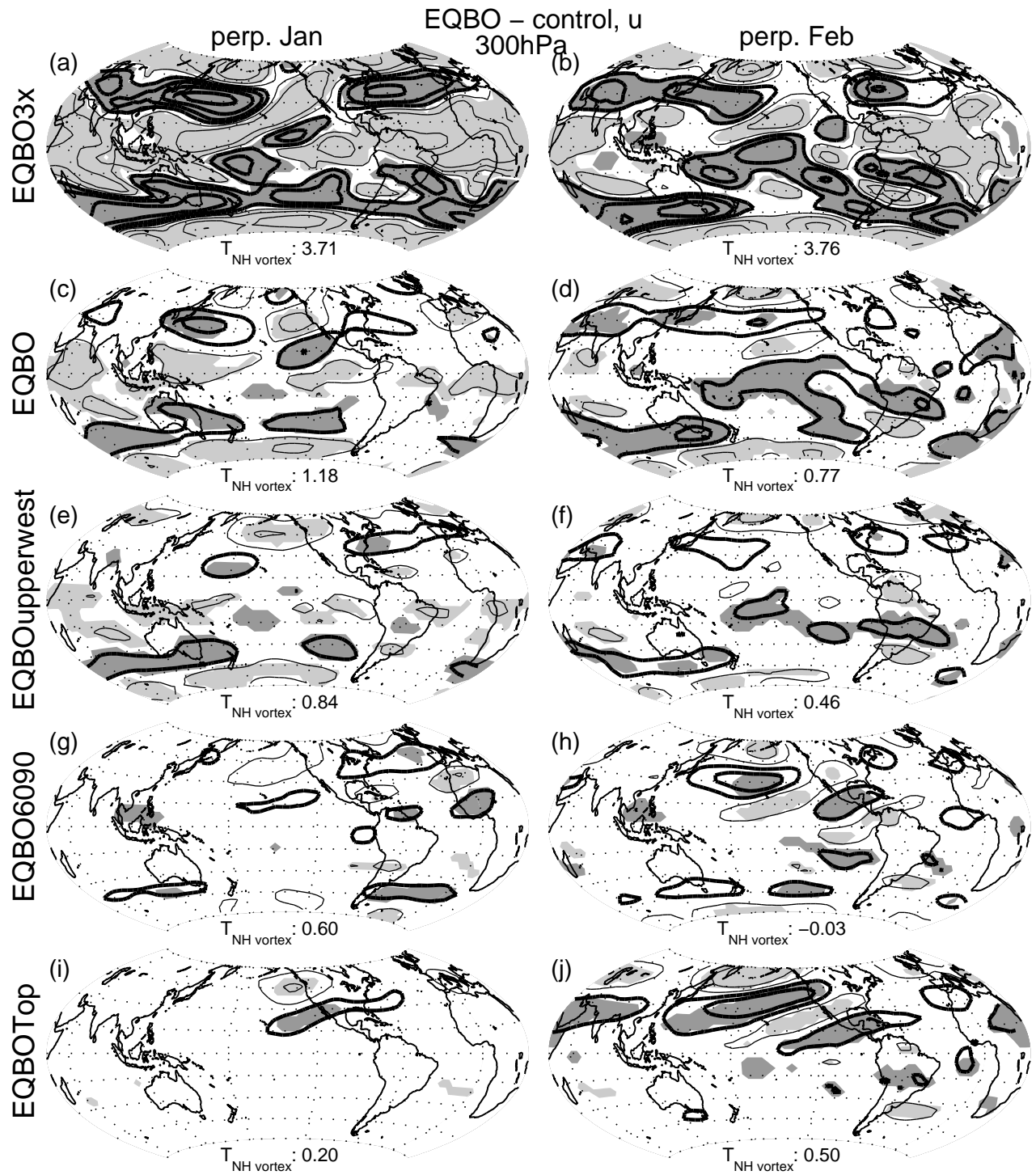


FIG. 11. Difference in zonal wind between the equilibrium EQBO cases and the FCONT and JCONT control cases for the different EQBO wind profiles. Below each panel is the difference in polar cap temperature (area averaged 70N and poleward from 70hPa to 150hPa) between each control case and the EQBO case. Contour interval like that in Figure 6. Significant regions at 95% are shaded and negative(easterly) contours are bolded.

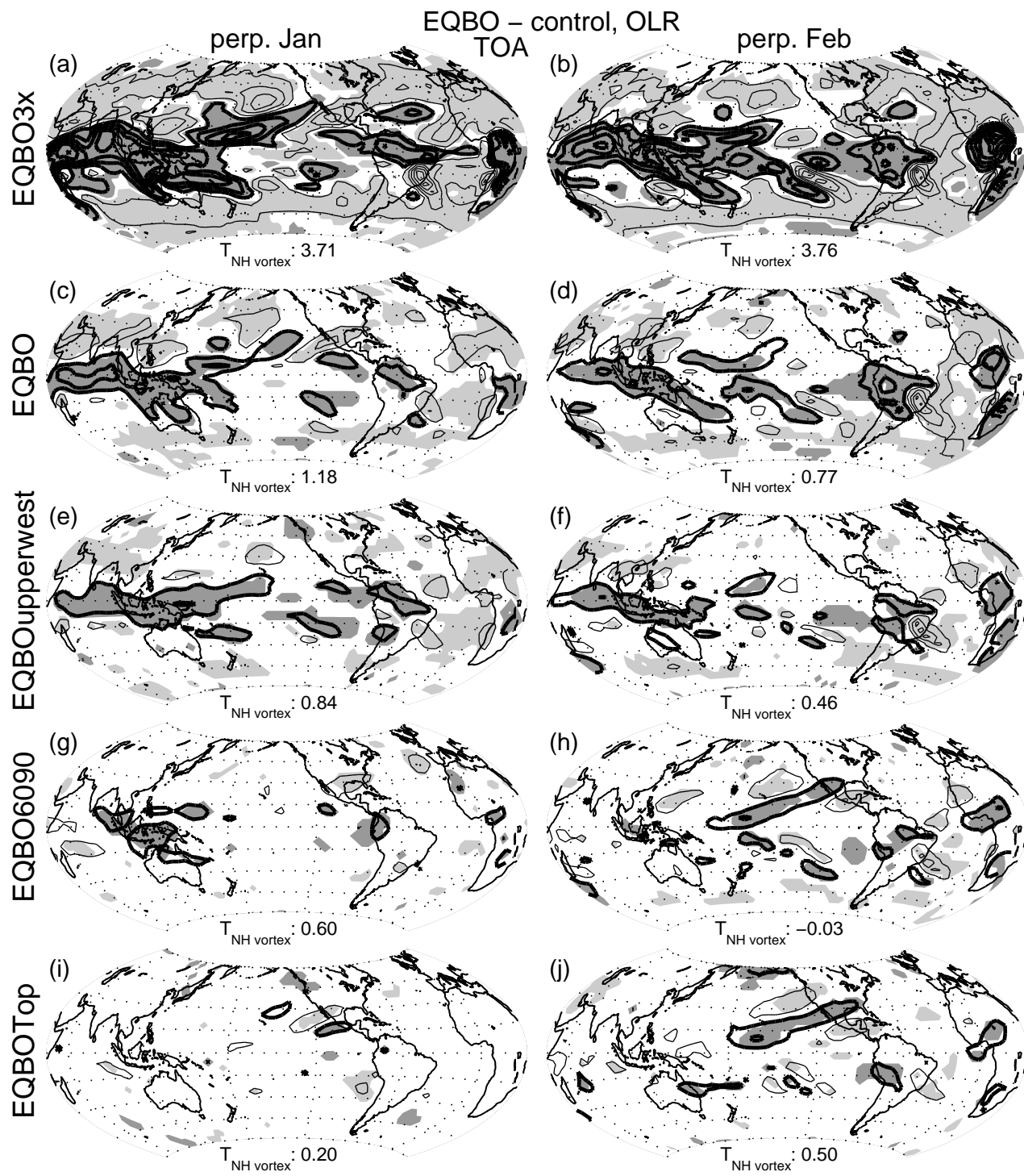


FIG. 12. Like Figure 11 but for OLR. Contour interval like that in Figure 8.